

FEA and Modal Analysis of a Damped Flywheel with Unbalanced Masses

Muhammad T. Hamisu*, Umar S. Umar and Aisha Sa'ad

Department of Mechanical Engineering, Nigeria Defence Academy, Kaduna, Nigeria

*Corresponding author: hmuhammادتukur@yahoo.com

Received 25 October 2019, Revised 19 November 2019, Accepted 27 November 2019.

Copyright © 2020 The Authors.

Abstract: In this paper, the complementary role of Finite Element Analysis (FEA) and Modal Analysis is studied using ANSYS Mechanical APDL. Primarily, two models (2D and 3D) of the flywheel are designed. Then, Finite Element (FE) static-stress analysis of the model was carried out, and it is found that the maximum von Mises stress (403 MPa) on the flywheel is lower than the yield stress (850 MPa) level, i.e. the design of the flywheel is safe. Afterwards, the Modal Analysis of the 3D model is carried out and six mode shapes are obtained at six different natural frequencies. Furthermore, Campbell diagram is plotted and two natural frequencies are identified. Moreover, mode shapes are plotted at the two critical speeds corresponding to their respective damped natural frequencies. The mode shapes are found to be stable, and therefore it can be remarked that the flywheel model is safe to operate within 12000 rpm. Finally, the performance of ANSYS models is determined by comparing analytical solution with the ANSYS results and the ANSYS solutions are accurate and robust.

Keywords: Finite element analysis; Flywheel; Modal analysis; Unbalanced mass.

1. INTRODUCTION

A flywheel is a mechanical device specially designed to efficiently store rotational energy as kinetic energy. Flywheels tend to resist changes in rotational speed due to their moment of inertia. The amount of energy stored in a flywheel is proportional to the square of its rotational speed and mass. The best way to change a flywheel's stored energy without varying its mass is by decreasing or increasing its rotational speed. Since flywheels act as mechanical energy storage devices, they are the kinetic-energy-storage devices thus analogous to electrical capacitors. Flywheels have found various applications in reciprocating engines, energy storage systems, gyroscopes, reaction wheels etc. [1]. Typically, an energy storage flywheel has a shaft with a rotor attached to it and a motor generator that can do the function of driving the shaft as well as extracting energy from it. It can deliver a large amount of energy in a short space of time. Typically, flywheels are made of steel and rotate on conventional bearings. These are largely limited to a maximum revolution rate of a few thousand rpm. Modern high energy density flywheels can be made of carbon fiber composites and employ magnetic bearings enabling them to revolve at speeds up to 60,000 rpm or higher. Some also use massive metal rotors but the rotational speed of these is limited by their ability to resist the high centrifugal forces. To keep energy losses to a minimum, most flywheels use magnetic bearings and operate in a vacuum chamber [1,2].

Vibrations are found in almost every rotating machine. Vibrations in rotating machines are due to mechanical faults which includes mass unbalance, mechanical looseness, coupling misalignment and many other causes. Unbalance is the common cause of vibration in machines. An unbalanced rotor would always cause more vibrations and would generate excessive force in the bearing area thereby reducing the life of the machine [3,4]. Largely, these vibrations are categorized as synchronous due to unbalance or non-synchronous due to self-excited rotor-whirling. The three main areas of utmost importance are the rotor critical speeds, system stability and unbalance response. Critical speeds are the undamped natural frequencies of the rotor system. As in any rotor design, the first step is to perform analysis that would determine the system critical speeds, mode shapes and energy distribution [4].

There has been numerous literature (experimentally, numerically and theoretically) on investigating stresses, mass unbalances, critical speeds, mode shapes and energy distribution of rotors in application. Bereznoi *et al.* [5] studied strain-stress state of a flywheel in kinetic energy storage. Abdul Saleem *et al.* [3] experimentally employed Shaft Detection Method in analyzing unbalances in rotating machines. The finding of this work provided a new method for detecting machinery unbalance, and offered a simplified approach for on-line fault detection in operating machinery. Deng *et al.* [6] investigated mass unbalances in a rotor system experimentally in a 3D space. They developed a non-contact method to identify unbalanced mass of rotor systems which consists a stereo video system along with a pair of synchronized high-speed cameras in order to substitute conventional contact transducer for measurement. The proposed method fared well when compared to the eddy

current method and laser displacement method and they provide more information than the conventional 2D detection methods. Kumar *et al.* [7] predicted shear stress and critical speed of a composite flywheel by varying different hub angles (4°, 5° and 0°) using Finite Element Method (FEM). The results showed hub angle of 4° had the maximum natural frequency along the flywheel profile and the nature of shear stress is minimum near its hub of the flywheel. Wang *et al.* [8] conducted a modal analysis on rotor-journal bearing system of a rotary compressor using the power spectral density map of the exciting forces on rolling piston via Fourier Transformation. The results showed that the first four orders of the exciting frequencies played a major role on the vibration of the system and the lateral as well as the torsional vibration mode were the major vibration modes of the system. Mutalikdesai *et al.* [9] performed modal analysis of a damped rotor using FEM. An FE code was written in MATLAB to obtain the eigenvalues, eigenvectors and modal damping factor. The study showed that during the forward whirl, damping decreases as the spin speed increases and in backward whirl, damping increases as the spin speed increases. By implementing this, the stability of the system was obtained.

Xu *et al.* [10] numerically simulated the vibration characteristics of unbalance response for motorized spindle system as a result of its complex structure and difficulty caused by unbalance in analyzing dynamic characteristics of the system. The results of both the theoretical result and numerical simulation showed that, when the speed and damping are constant, the steady-state unbalance response of the motorized spindle system go through harmonic vibration with the same frequency as the rotating speed, and the amplitude of the vibrations is directly proportional to the mass of the unbalance. Liu *et al.* [11] theoretically studied the vibration analysis on 600 Wh Energy Storage Flywheel Rotor with an active Magnetic Bearing System based on simplified rotor dynamic model. The whirl frequency was calculated under different parameters of the controller in MATLAB to understand its effect on the whirl frequency and to limit the operating speed as well as acceleration or deceleration of the rotor, and as such, the Campbell Diagram was obtained accordingly. The results informed that it can be applied in understanding the right position to set the rotor system support, limit the ratio of transverse moment of inertia and guide in future design of a flywheel prototype. Gutierrez-Wing [12] proposed a new method for the modal characterization of rotating machinery structures. The new method is based on the modelling of rotating machines as structural assemblies of rotating and non-rotating components and it accounts for the effects of gyroscopic and other forces related to rotation. By comparison with conventional methods with the same feature, the new method has the improvement that it does not involve the measurement of a whole row of the frequency response function (FRF) matrix.

Bhuyan *et al.* [13] implemented Timoshenko Beam Elements Theory using FEM to study the modal characteristics of a flexible rotor system having two non-identical discs mounted on it. The gyroscopic effect was seen to be noticeable at higher rotating speeds for both cases which caused the frequency pairs to split into backward and forward whirls. The Campbell diagram was computed which helped in defining the critical speeds connected to each pair of diverging natural frequencies. Similarly, Zhu *et al.* [14] applied Timoshenko Beam Elements Theory using FEM to analyze the dynamics of a damped rotor-bearing system subject to base vibrations or excitations. It was discovered the base excitation frequency near the natural frequency of the rotor affects both the rotor vibration in the direction of excitation and the rotor oscillation in the other directions. El-Saeidy *et al.* [15] investigated dynamics of a rigid rotor linear and non-linear bearing systems that is subjected rotational imbalance and base excitation. The rotor-linear bearing system employed numerical integration using the Runge–Kutta method and typical agreement was obtained when compared to analytical solutions. For the rotor-linear bearing system, results are obtained from numerical integration and discussed with regards to the fast Fourier transform (FFT), time domain, and Poincaré map. The frequency response was characterized by peaks at natural frequencies of the rotating gyroscopic system.

Based on the available and non-exhaustive collection of literatures presented above on rotor dynamics, there are few literatures where the applications of FEA and Modal Analysis are studied therein. In this paper, the objective is to study the properties and procedures of FEA and Modal Analysis in order to appreciate the merits and demerits of both techniques and to study the interrelationship and complementary role between these methods [16].

2. METHODOLOGY

2.1 Problem Description

This study represents FE-based static stress analysis of a flywheel in order to evaluate the stress level developed in the flywheel at the maximum rotational speed under action of the inertial loads due to the rotor rotation. Moreover, modal analysis is going to be carried out in order to identify whether the flywheel will not operate dangerously close to the resonance within the operating rotational speed 12000 rpm (assumption made on the lower side of flywheel rotational speeds), and to determine whether it is likely to pass through the resonances under speeding-up the flywheel to the nominal operation speed. It is also assumed that the flywheel lateral displacements are constrained at the roller-bearing supports. The vertical displacements are constrained at the bottom end flywheel surface.

To achieve the objectives, modal analysis has to be performed to determine the natural mode shapes and natural frequencies of an object during free vibration. Modal analysis in ANSYS Mechanical APDL is a linear analysis. To find the natural frequencies and mode shapes Eigen problem have to be solved.

$$K\phi_j = \omega_j^2 M\phi_j \quad (1)$$

where K and M are stiffness and mass matrix respectively, ω_j and ϕ_j are j -th natural frequency and mode shape. In this study Damped method was used since this problem is related to rotor dynamics in stationary frame with damping via bearings at both ends of the flywheel. Eigen problem with damping and or Coriolis forces [17,18,19]

$$\omega^2 [M]\{\phi\} + \omega [C]\{\phi\} + [K]\{\phi\} = 0 \quad (2)$$

If ϕ_j is a mode then $C\phi_j$ shape (C is any number) is also a mode shape. Mode shapes does not give absolute values for displacement but only the values about ratios between stresses, strains and displacements at different locations as a result. Mode shapes are often subjected to normalization: is chosen in a way to satisfy special conditions. Most common condition for normalization are: Mass Normalization where the mode shape is normalized to satisfy $\phi_j^T M \phi_j = 1$ and Unit Displacement Normalization where the maximum component in the mode shape vector ϕ_j is chosen to be 1 [17].

2.2 Design Considerations

The FEA of the flywheel is carried out according to the provided specifications and AutoCAD generated IGES file as can be seen in Figure 1. Then the model is imported into ANSYS Mechanical APDL for static-stress analysis and modal analysis. The material is stainless steel and other important parameters are given in Table 1. Therefore,

$$\omega = \frac{2\pi N}{60} = \frac{2\pi(12000)}{60} = 1256.64 \quad (3)$$

where ω = Angular velocity (rad/s) and N is in rpm.

2.3 Building of the Models

2.3.1 2D Model for Static Stress Analysis

The building of the flywheel model for static stress analysis is carried out in ANSYS Mechanical APDL. Since the structure of the flywheel is axisymmetric, therefore it can be modelled as a 2D model for static stress analysis. By following standard procedure, the model of flywheel was created as per required specification which is shown in Figure 1.

2.3.2 3D Model for Modal Analysis

The flywheel model for modal analysis is designed in ANSYS Mechanical APDL by sweeping the 2D mode of the flywheel around the axle centerline. The 3D model of the flywheel is shown in Figure 2.

2.4 Mesh Generation and Mesh Independence Study

2.4.1 Static-Stress Analysis

For static stress-analysis under the action of centrifugal forces, FE mesh is created on the 2D flywheel model. Before mesh, load is applied on the model, zero structural displacement applied on the bottom end of the flywheel, $UY = 0$ and zero structural displacement, $UX = 0$ is applied on both ends of the flywheel at the locations of roller bearings as circled in Figure 3. Centrifugal force with rotating speed 1256.64 rad/s is applied in y -axis i.e. on the left hand side edge of cross-sectioned flywheel. Table 2 shows the mesh specifications refinement (coarse to fine) from mesh A to mesh H . In order to check mesh independence, maximum von Mises stress of the 2D flywheel model under the action of centrifugal forces is plotted in the histogram as show in Figure 4 since variation of the maximum von Mises stress is not significant after mesh E , so it is certain that the mesh has converged.

Table 1. Design parameters

Parameter	Value
Young's modulus	140 GPa
Poisson ratio	0.28
Yield strength stress	850 MPa
Density	4400 kg/m ³
Operating speed range	0 – 12000 rpm
Angular Velocity	1256.64 rad/s

Table 2. Specifications of different meshes for the 2D model

Mesh	Specification	Number of Elements
A	Smart Size 4	350
B	Smart Size 2	875
C	Smart Size 4, Refine at 1	1400
D	Smart Size 2, Refine at 1	3500
E	Smart Size 1, Refine at 1	5,132
F	Smart Size 1, Refine at 2	11,547
G	Smart Size 1, Refine at 3	20,528
H	Smart Size 1, Refine at 4	82,112

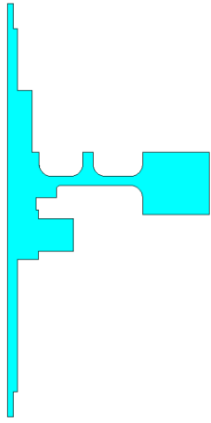


Figure 1. Flywheel 2D Model

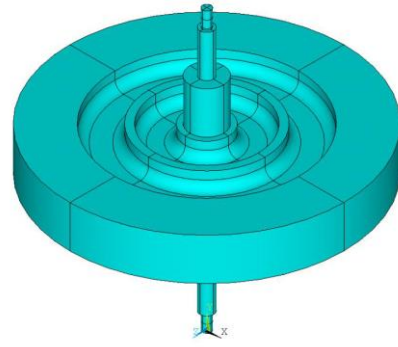


Figure 2. Swept flywheel 3D model

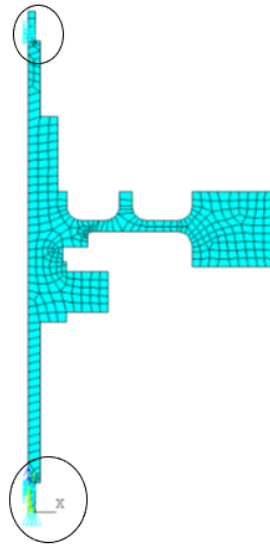


Figure 3. Structural displacements

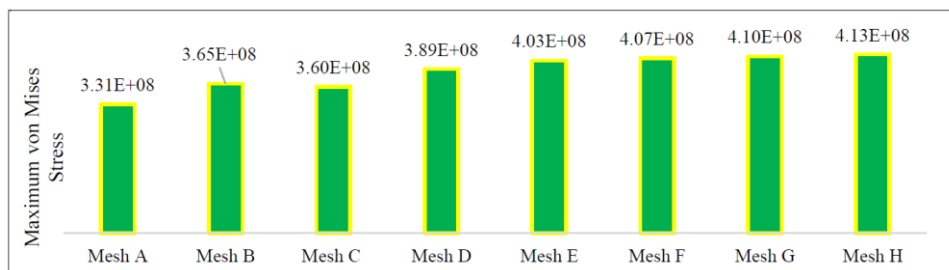


Figure 4. Maximum von Mises Stress on the 2D flywheel model with different FE mesh sizes

2.4.2 Modal Analysis

The same procedure applied in static-stress analysis is upheld here. In order to check for the mesh independence, frequencies with different FE mesh sizes of the flywheel model is plotted in 3D Line diagram shown in Figure 5 and it can be seen that all the four lines for different mesh sizes are following same trend. From the plot, it is certain that mesh has converged and independent.

3. RESULTS AND DISCUSSION

3.1 Static Stress Analysis of the Flywheel

The 2D model of the flywheel was analyzed using Mesh E and the distribution of von Mises stress over the flywheel model is shown in Figure 6. It is found that, the maximum stress on the flywheel is $4.03 \times 10^2 \text{ N/m}^2$, the minimum stress is $2.95 \times 10^3 \text{ N/m}^2$ and maximum displacement of the flywheel is $1.92 \times 10^{-4} \text{ m}$. From the static stress analysis of the flywheel under centrifugal force, it can be seen that the design of the flywheel is completely safe since the maximum stress on the flywheel

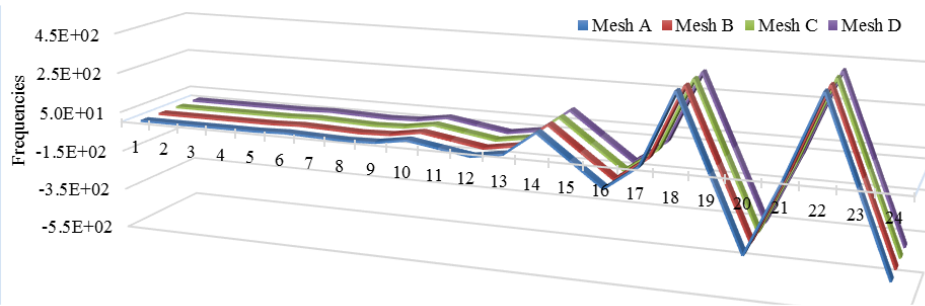


Figure 5. 3D plot for natural frequencies with different mesh sizes of the 3D flywheel model

(403 MPa) is lower than the yield stress level (850 MPa). It signifies that there is no possibility of fracture of the material even in maximum stress concentrated areas of the flywheel model which is on the rotor.

3.2 Modal Analysis of the Flywheel

After the simulation, six mode shapes were obtained from the first six natural frequencies. Each natural frequency has a corresponding unique 'mode-shape' with different parts of the flywheel vibrating at different amplitudes and differing phases relative to one another. The ratio of bearing stiffness to shaft stiffness has a strong impact on mode shapes. Different mode (deformed and undeformed) with respect to chosen natural frequencies can be seen in Figures 7-9. Mode shape 1 corresponding to first natural frequency is stable or rigid which resembles the torsional natural mode. It has zero value as the torsional rigid body motion is not constrained, with insignificant deflection of shaft or the structure. On the other hand, mode shape 2 and mode shape 5 are backward (BW) stable, i.e. the flywheel rotates on the whirl orbit with the opposite direction as about the rotational velocity. Also, mode shape 3, mode shape 4 and mode shape 6 are forward (FW) stable i.e. the flywheel rotates on the whirl orbit with the same direction as about the rotational velocity. These classifications of vibrational modes in terms of FW stable, BW stable and stable can be clearly observed in the Campbell diagram in Figure 10. In order to identify 'critical speeds' or 'peak response speeds' at resonance, and also to observe how a wider range of shaft speeds changes the situation, modal analysis was performed with a range of shaft speeds viz. 100 rad/s, 628 rad/s and 1256 rad/s. The obtained natural frequencies from modal analysis is shown in Figure 11 and it can be understood that how natural frequencies increase with higher operating speeds of the flywheel.

Furthermore, damped natural frequencies (in terms of forward whirl and backward whirl) are plotted against rotational speed (1X) i.e. the unbalance excitation frequency, in the Campbell diagram by using ANSYS Mechanical APDL. From the Campbell diagram, it is found that the forward whirling natural frequency increases with increase in rotational speed, because as the shaft speed increases, the gyroscopic effects essentially act like an increasingly stiff spring on the central disk for the rocking motion. Increasing stiffness acts to increase the natural frequency. On the other hand, whirling natural frequency decreases with the increase in rotational speed of the flywheel, since increasing rotor spin speed acts to reduce the effective stiffness, thus reducing the natural frequency. Therefore, the forward modes increase in frequency with increasing speed, while the backward modes decrease in frequency with increasing speed. How much the mode changes depend on the distribution of mass and diametric mass moment of inertia and the shape of the corresponding mode shape [20,21].

The system is said to be "in resonance" when the excitation frequency i.e. the spin velocity matches the damped natural frequency, at resonance amplitude of vibration is higher. Critical speeds occur at the point of resonance i.e. the peak response speed when a system natural frequency is excited by the rotor unbalanced masses [20,21]. From the Campbell diagram, three speeds (N1, N2 and N3) were identified as where unbalance excitation frequency intersects with damped natural frequencies. Among these three speeds, N1 and N2 are critical speeds, but N3 is not a critical speed. Since unbalance does not excite the backward modes in the flywheel rotor-bearing system, there are no critical speeds corresponding to the intersections between the spin velocity line and backward modes. That is, at N3, the steady state unbalance response curve shows no phase shift and no peak [20-22]. When the flywheel experiences high vibration at 1X spin, the first course of action is to improve the balance of the rotor. The reason behind balancing the rotor is to ensure that flywheel is safe and reliable. There are various ways to the balancing, one of which is modal balancing. Thus, an acceptable balance limit must be set for long term reliability to be achieved without unnecessary expense of extreme balancing procedures. A rotor balance quality or procedure of G6.3 can be used for the flywheel [23].

Therefore, two critical speeds are $N1 \approx 685$ rad/s and $N2 \approx 148$ rad/s with corresponding natural frequencies 110 Hz, and 24 Hz respectively. (N.B. – these values are approximate value taken from the Campbell diagram). From the Campbell diagram, it is also found that, all six natural frequencies are either FW stable or BW stable or stable; there is no unstable frequency. Therefore, the flywheel model is safe to operate within the speed range of 0 to 1256 rad/s. In order to plot the mode shapes at critical speeds, two other simulations were performed at 685 rad/s and 148 rad/s. Then mode shapes were subsequently plotted at corresponding frequencies of critical speeds taken from Campbell diagrams of the flywheel. Different mode shapes at two critical speeds are shown in Figure 12.

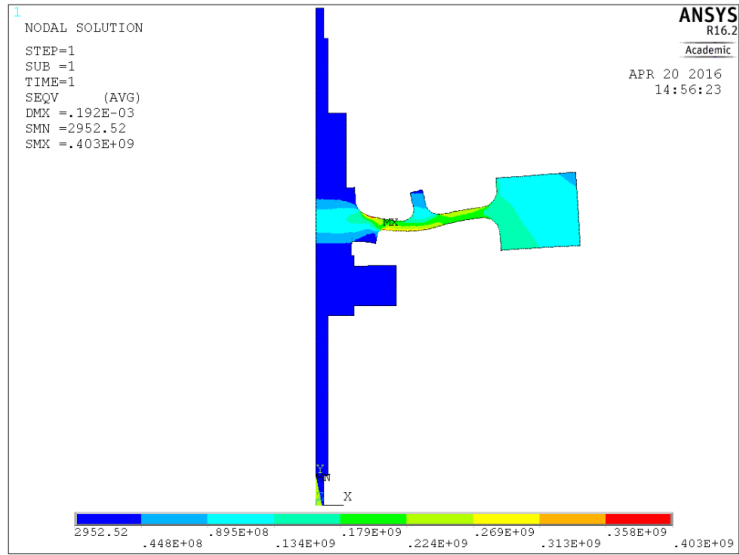


Figure 6. von Mises stress over the cross section of the flywheel

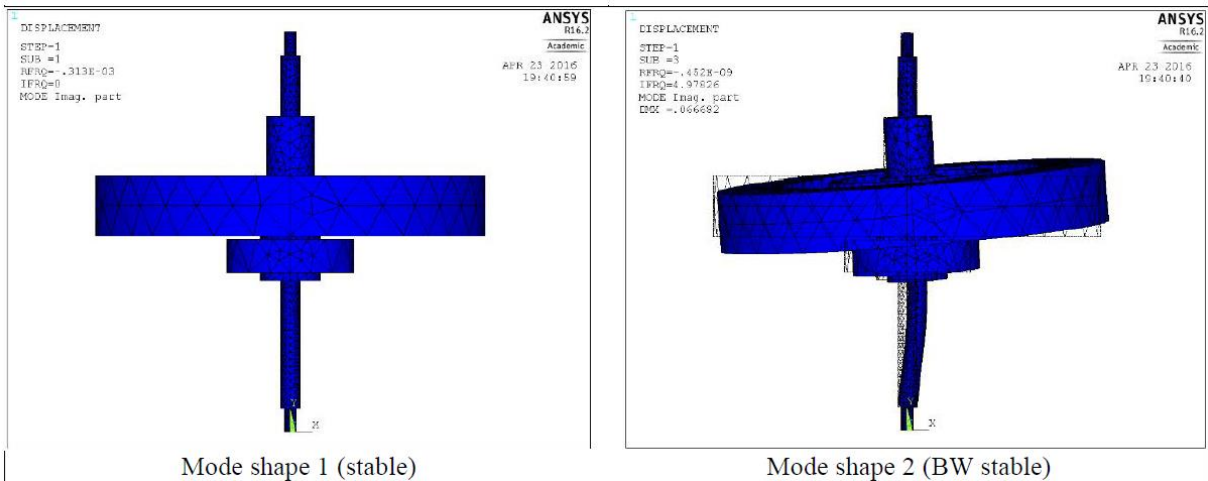


Figure 7: First and second mode shapes

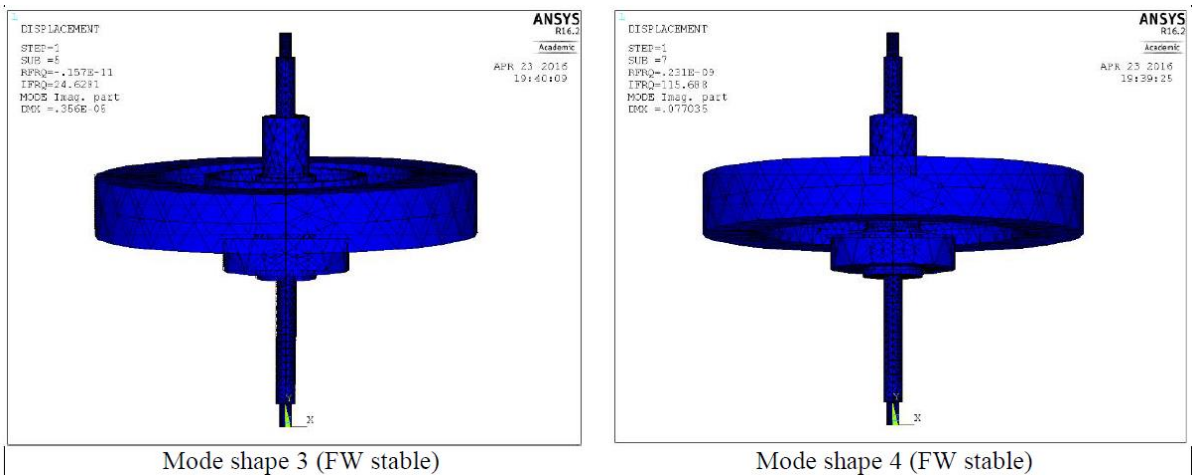


Figure 8. Third and fourth mode shapes

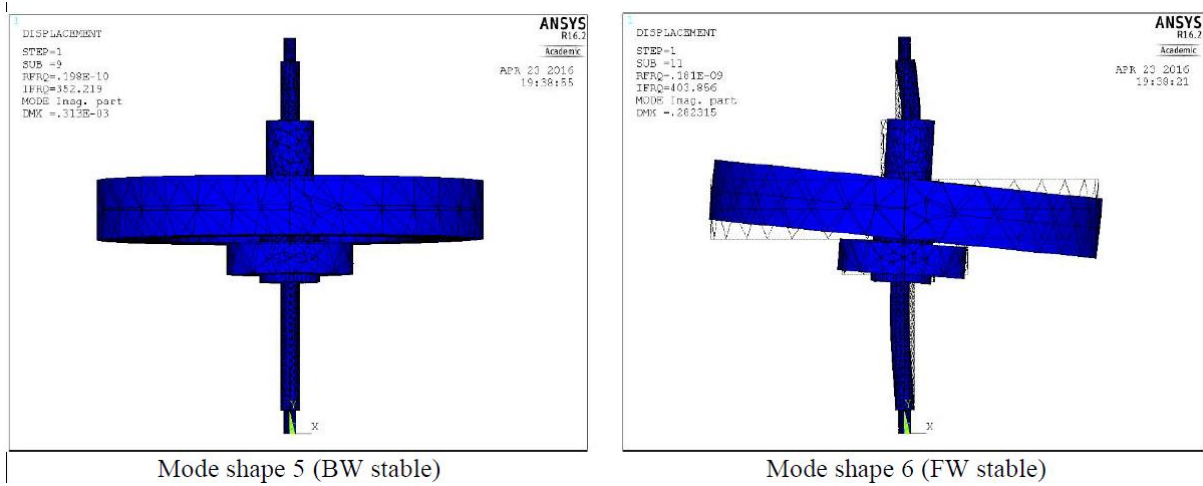


Figure 9. Fifth and sixth mode shapes

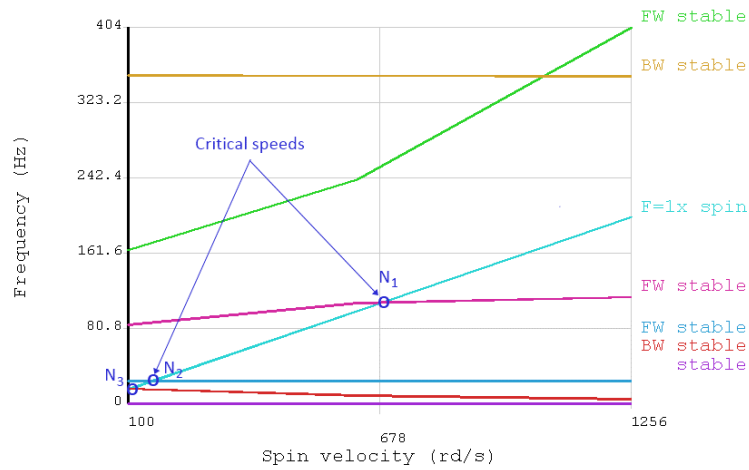


Figure 10. Campbell diagram of the flywheel model

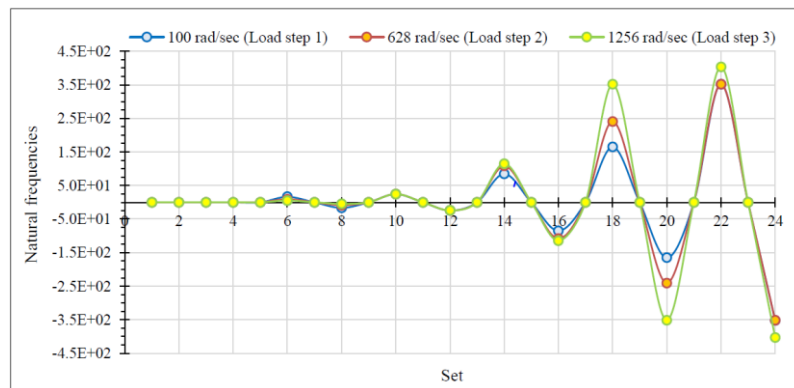


Figure 11: Variation of natural frequencies with different rotational speeds

3.3 Verification and Validation

3.3.1 Analytical Solutions

The calculations of the analytical solutions for the von Mises stress throughout the rim of the flywheel is shown in this subsection. From the ANSYS, we can find inner and outer radius of the disc as shown in Figure 13(A). Therefore, $r_1 = 0.196$ m, $r_2 = 0.0732$ m. The von Mises or equivalent tensile stress throughout the rim of the flywheel disc can be calculated as follows [24]:

$$\sigma_t = \rho \times r^2 \times \omega^2 = \rho \times (r_1^2 - r_2^2) \times \omega^2 \tag{4}$$

where σ_t is the von Mises stress or equivalent tensile stress, r is the radius of the disc, r_1 is outer radius of the disc, r_2 is inner radius of the disc and ω is the angular velocity. The von Mises stress can be found as

$$\sigma_t = 4400 \times (0.196^2 - 0.0732^2) \times 1256.636^2 = 1.0477 \times 10^8 \text{ Pa} \quad (5)$$

In order to compare analytical solution with the ANSYS results, a path (A-B) was created along the rim of the flywheel disc as shown in Figure 13(B). von Mises stress along the rim of the flywheel disc is shown in Table 3.

3.3.2 Comparison between Analytical and Predicted Results

To verify the reliability of the simulation, analytical solutions were compared with ANSYS based predicted results. Comparisons of predicted and analytical solutions for ANSYS model is shown in Figure 14. In this figure, the average von Mises stress (taken from ANSYS) along the rim of the flywheel disc is compared with the analytical solution. From the Figures, it is certain that the performance of ANSYS model very decent and reliable. The differences between the analytical results and numerical results are referring to the fact that the numerical results have numerical errors and those errors could come from many different sources such as the boundary conditions.



Figure 12. (A) Mode shape at critical speed N1 (685 rad/s, 109.56 Hz & FW stable) and (B) Mode shape at critical speed N2 (148 rad/s, 24.47 Hz & FW stable)

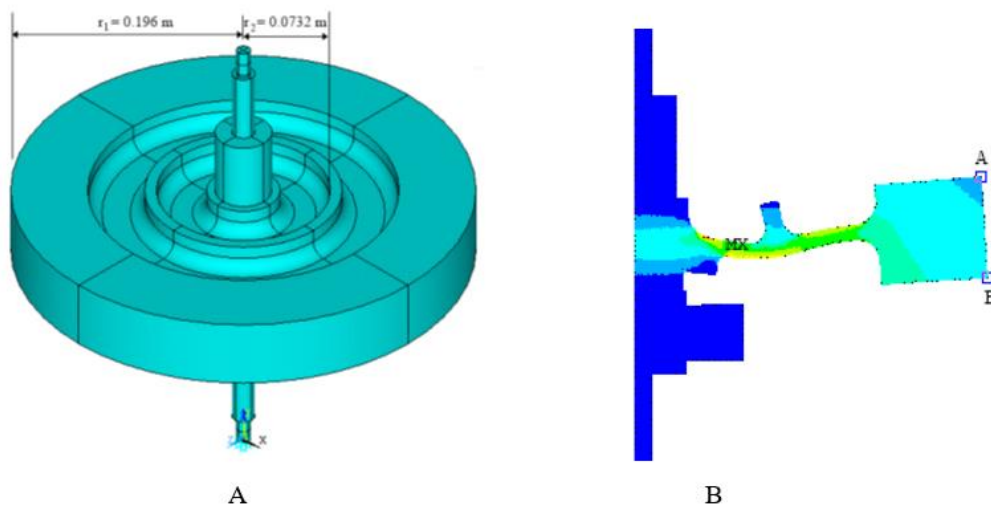


Figure 13. (A) Flywheel model showing disc dimensions; (B) Flywheel model showing path A-B along the rim

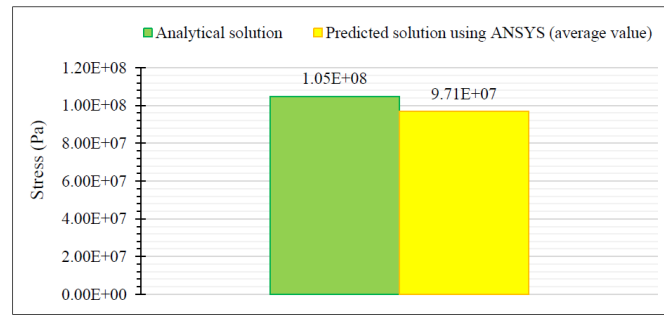


Figure 14. Comparison of analytical solutions with ANSYS results

Table 3. Stress along the rim of the flywheel (Average von Mises stress = 9.71×10^7 Pa)

Distance along the rim of the flywheel disc (m) $\times 10^{-3}$	0	3.00	6.00	9.00	12.00	15.00	18.00	21.00	24.00
von Mises stress (Pa) $\times 10^7$	8.33	8.48	8.63	8.78	8.93	9.07	9.22	9.36	9.50
Distance along the rim of the flywheel disc (m) $\times 10^{-3}$	27.00	30.00	33.00	36.00	39.00	42.00	45.00	48.00	51.00
von Mises stress (Pa) $\times 10^7$	9.64	9.77	9.90	10.00	10.10	10.30	10.40	10.50	10.60
Distance along the rim of the flywheel disc (m) $\times 10^{-3}$	54.00	57.00	60.00						
von Mises stress (Pa) $\times 10^7$	10.70	10.80	10.90						

4. CONCLUSION

The FEA gave an insight on the flywheel model that it can safely operate within the range of 0 to 12000 rpm as it was found that the maximum von Mises stress (403 MPa) on the flywheel is lower than the yield stress (850 MPa). Also, FEA model of the flywheel model is decidedly successful to analyze the flywheel model with a higher degree of exactitude. The results from the Modal Analysis presented the basic dynamic properties (mode shapes and natural frequencies) of the flywheel. Similarly, with the help of the Campbell Diagram, the critical speeds $N1 \approx 685$ rad/s and $N2 \approx 148$ rad/s with corresponding natural frequencies 110 Hz and 24 Hz respectively were identified. In case of any anomaly, these properties can then be used directly in a FE model of the flywheel, for subsequent problem solving or re-designing the equipment for more optimum dynamic response.

From the results obtained, it is evident that FEA and Modal Analysis are complementary in understanding the structural dynamics of rotating machineries. However, the main assumption involved in the acquisition of this information is that the structural system is linear, i.e., structural displacements are directly proportional to applied loads. In practical structures, this condition is not always the case and therefore, structural systems may be non-linear to some degrees. To account for this non-linearity, it is recommended for further work, even though most linear structural dynamics problems may now be solved accurately and less expensive. Typically, in such cases, a solution strategy is usually implemented on a case-by-case basis and the structural geometry as well as the elasticity may be needed in significant details to input the data. Conclusively, in designing a rotating structure, it is intuitive to start performing a static-stress analysis followed by modal analysis, and then other dynamic analyses (harmonic, transient etc.)

ACKNOWLEDGMENT

The authors would like to thank the staff of University of Sussex at the Department of Mechanical Engineering Cluster Room for their IT support in carrying out the numerical analyses.

REFERENCES

- [1] P. Breeze, *Power System Energy Storage Technologies*, Cambridge Massachusetts: Academic Press, Elsevier Ltd., 2018.
- [2] Breakthrough in Ricardo Kinergy 'second generation' high-speed flywheel technology. <https://ricardo.com/news-and-media/news-and-press/breakthrough-in-ricardo-kinergy-%e2%80%98second-generation> (accessed 15.10.2019).
- [3] M. D. Abdul-Saleem, G. Diwakar and M. R. S. Satyanaranaya, Detection of unbalance in rotating machines using shaft deflection measurement during its operation, *Journal of Mechanical and Civil Engineering*, 3(3), 8-20, 2012.
- [4] E. J. Gunter, Introduction to Rotor Dynamics, Critical speed and unbalance response analysis. https://dyrobes.com/wp-content/uploads/2016/04/Introduction-to-Rotor-Dynamics-Critical-Speed-and-Unbalance-Response-Analysis-E.-J.-Gunter_linked.pdf (accessed 17.10.2019).
- [5] D. V. Berezhnoi, D. E. Chickrin, L. R. Gajnulina, E. Y. Kurchatov, P. A. Kokunin, I. G. Sozutov and M. I. Shigapov, Calculation of strain-stress state of flywheel in potential field, *Contemporary Engineering Sciences*, 8(36), 1703-1712, 2015.

- [6] H. Deng, Y. Diao, J. Zhang, P. Zheng, M. Ma, X. Zhong and L. Yu, Three-dimensional identification for unbalanced mass of rotor systems in operation, *Applied Sciences*, 8(173), 1-14, 2018.
- [7] G. Kumar, A. K. Jain and S. G. Meena, Prediction of shear stresses and critical speed of composite flywheel by varying different hub angles using FEM, *Journal of Emerging Technologies and Innovative Research*, 4(10), 40-46, 2017.
- [8] Z. L. Wang, Q. K. Feng, F. Y. Zhang and X. L. Yu, Modal analysis of the rotor, *International Compressor Engineering Conference*, Purdue, 2012, pp. 1-8.
- [9] P. Mutalikdesai, S. Chandraker and H. Roy, Modal analysis of damped rotor using finite element method, *National Conference on Advances in Modelling and Analysis of Aerodynamic Systems*, Odisha, 2013, pp. 98-103.
- [10] J. Xu, X. Zheng, J. Zhang and X. Liu, Vibration characteristics of unbalance response for motorized spindle system, *13th Global Congress on Manufacturing and Management*, China, 2017, pp. 331-340.
- [11] J. Liu, Z. Ren, S. Wu and Y. Tang, Theoretical vibration analysis on 600 Wh energy storage flywheel rotor - Active magnetic bearing system, *International Journal of Rotating Machinery*, 512674, 1-11, 2013.
- [12] E. S. Gutierrez-Wing, *Modal analysis of rotating machinery structures*, PhD Dissertation, Mechanical Engineering, Imperial College London, 2003.
- [13] A. Bhuyan and R. Verma, The modal analysis of a double disc flexible rotor-bearing system with isotropic stiffness and damping properties, *Journal of Physics - Conference Series*, 1240(1), 1-8, 2019.
- [14] H. Zhu, W. Chen, R. Zhu, J. Gao and M. Liao, Study on the dynamic characteristics of a rotor bearing system with damping rings subjected to base vibration, *Journal of Vibration Engineering & Technologies*, 7(1), 1-12, 2019.
- [15] F. M. A. El-Saeidy and F. Sticher, Dynamics of a rigid rotor linear/nonlinear bearings system subject to rotating unbalance and base excitations, *Journal of Vibration and Control*, 16(3), 403-438, 2010.
- [16] N. F. Rieger, The relationship between finite element analysis and modal analysis. <https://pdfs.semanticscholar.org/2e09/f264d152bacc101062de808aa086840bb840.pdf> (accessed 23.10.2019).
- [17] Ansys Inc, Rotor analysis guide. https://www.academia.edu/25880155/Rotordynamic_Analysis_Guide (accessed 23.10.2019).
- [18] M. B. Wagner, A. Younan, P. Allaire and R. Cogill, Model reduction methods for rotor dynamic analysis - A survey and review, *International Journal of Rotating Machinery*, 10, 1-17, 2010.
- [19] H. C. Jung and S. Krumdieck, Rotordynamic modelling and analysis of a radial inflow turbine rotor-bearing system, *International Journal of Precision Engineering and Manufacturing*, 15(11), 2285-2290, 2004.
- [20] F. C. Nelson, Rotor dynamics without equations, *International Journal of COMADEM*, 10(3), 2-10, 2007.
- [21] E. Swanson, C. D. Powell and S. Weismann, A practical review of rotating machinery critical speeds and modes, sound and vibration. <http://www.sandv.com/downloads/0505swan.pdf> (accessed 23.10.2019).
- [22] F. Kushner, R. A. Strickland and J. Sharina, Rotating component modal analysis and resonance avoidance recommendation - An update, *Proceedings of the 42nd Turbomachinery Symposium*, Texas Houston, 2013, pp. 1-24.
- [23] T. D. Feese and P. E. Grazier, Balance this! Case histories from difficult balance jobs, *Proceedings of 33rd Turbomachinery Symposium*, Texas Houston, 2004, pp. 1-22.
- [24] Roymech, Flywheel basics. https://roymech.org/Useful_Tables/Cams_Springs/Flywheels.html (accessed 23.10.2019).